A systems biology approach identifies the biochemical mechanisms regulating monoterpenoid essential oil composition in peppermint

Rigoberto Rios-Estepa*†, Glenn W. Turner*, James M. Lee†, Rodney B. Croteau*‡, and B. Markus Lange*‡§¶

*Institute of Biological Chemistry, §M. J. Murdock Metabolomics Laboratory, ¶Center for Integrated Biotechnology, and †School of Chemical Engineering and Bioengineering, Washington State University, Pullman, WA 99164-6340

Contributed by Rodney B. Croteau, December 29, 2007 (sent for review November 21, 2007)

The integration of mathematical modeling and experimental testing is emerging as a powerful approach for improving our understanding of the regulation of metabolic pathways. In this study, we report on the development of a kinetic mathematical model that accurately simulates the developmental patterns of monoterpenoid essential oil accumulation in peppermint (*Mentha* × *piperita*). This model was then used to evaluate the biochemical processes underlying experimentally determined changes in the monoterpene pathway under low ambient-light intensities, which led to an accumulation of the branchpoint intermediate (+)-pulegone and the side product (+)-menthofuran. Our simulations indicated that the environmentally regulated changes in monoterpene profiles could only be explained when, in addition to effects on biosynthetic enzyme activities, as yet unidentified inhibitory effects of (+)-menthofuran on the branchpoint enzyme pulegone reductase (PR) were assumed. Subsequent *in vitro* analyses with recombinant protein confirmed that (+)-menthofuran acts as a weak competitive inhibitor of PR (K_i = 300 μM). To evaluate whether the intracellular concentration of (+)-menthofuran was high enough for PR inhibition *in vivo*, we isolated essential oil-synthesizing secretory cells from peppermint leaves and subjected them to steam distillations. When peppermint plants were grown under low-light conditions, (+)-menthofuran was selectively retained in secretory cells and accumulated to very high levels (up to 20 mM), whereas under regular growth conditions, (+)-menthofuran levels remained very low (<400 μM). These results illustrate the utility of iterative cycles of mathematical modeling and experimental testing to elucidate the mechanisms controlling flux through metabolic pathways.

kinetic modeling | monoterpene biosynthesis | isoprenoid | menthofuran | pulegone reductase

The commercially valuable essential oil of peppermint (*Mentha* × *piperita*) consists primarily of *p*-menthane-type monoterpenes (1), which are synthesized and accumulated in leaf protuberances termed peltate glandular trichomes (2, 3). Within these trichomes, the biosynthesis of monoterpenes is restricted to nonphotosynthetic secretory cells that are arranged in an eight-celled disk (4). The secretory cells exude essential oil into an emerging cavity formed by the separation of a preformed layer of cuticular material (5). Modification of a general protocol for the isolation of peppermint secretory cells (6) enabled the extraction of high-quality mRNA, the generation of cDNA libraries, the sequencing of randomly selected clones, and the functional testing of cDNAs by expression of recombinant proteins in microbial hosts (7). In combination with developmental studies at the microscopic, molecular, and biochemical levels, these functional genomics approaches have yielded a wealth of information about the biochemical properties of the individual biosynthetic enzymes and the regulation of the monoterpene pathway as a whole (reviewed in ref. 8).

In peppermint secretory cells, the precursors of monoterpenes are derived exclusively from the leucoplast-localized mevalonate-independent pathway (9, 10). The first committed step of the monoterpene pathway, the conversion of geranyl diphosphate to (−)-limonene, is catalyzed by (−)-limonene synthase (11, 12), which is also localized to leucoplasts (13) (Fig. 1). After translocation to the endoplasmic reticulum, (−)-limonene undergoes a cytochrome P450-dependent hydroxylation, catalyzed by (−)-limonene 3-hydroxylase (14), to form (−)-transisopiperitenol. After import into mitochondria, (−)-transisopiperitenol is oxidized to (−)-isopiperitenone by a specific NAD^+-dependent short-chain dehydrogenase (15, 16). A double-bond reduction, catalyzed by (−)-isopiperitenone reductase (17), followed by an isomerization of (+)-*cis*-isopulegone (18) generates the branchpoint intermediate (+)-pulegone in the cytosol. Cytosolic (+)-pulegone reductase (PR) synthesizes both (−)-menthone and (+)-isomenthone from (+)-pulegone (17). Further conversions in the main monoterpene pathway are catalyzed by the bifunctional cytosolic activities of (−)-menthone:(−)-(3*R*)-menthol reductase and (−)-menthone:(−)-(3*S*)-neomenthol reductase (19). The side product (+)-menthofuran can be formed from (+)-pulegone by the action of (+)-menthofuran synthase (MFS), an endoplasmic reticulum-localized cytochrome P450-dependent monooxygenase (20). The highest rates of monoterpene biosynthesis were measured during the period of maximal leaf expansion (12–20 days after leaf initiation) (21). Based on $^{14}CO_2$ incorporation experiments with subsequent radio-GC analysis, the rate of monoterpene biosynthesis appeared to be the most important factor controlling leaf monoterpene levels. Subsequent studies established that the transcript levels of genes involved in the peppermint monoterpene pathway and the corresponding enzyme activities correlated well with the rate of monoterpene biosynthesis (22), indicating that flux might be coordinately regulated at the level of gene expression.

High-quality oils are characterized by a complex compositional balance of monoterpenes with high (−)-menthol, moderate (−)-menthone, and low (+)-pulegone and (+)-menthofuran quantities (23, 24). Under adverse environmental conditions, such as low light intensity, water deficit, and/or high night temperatures, elevated quantities of (+)-pulegone and (+)-menthofuran accumulate (25, 26), thus rendering an oil of unsatisfactory quality. Mahmoud and Croteau reported that transgenic plants with decreased MFS transcript levels accumulated vastly reduced (+)-pulegone and (+)-menthofuran amounts under regular and stress conditions (27). Further studies indicated that PR transcript levels decreased in the

Author contributions: R.R.-E., G.W.T., and B.M.L. designed research; R.R.-E. and G.W.T. performed research; R.R.-E., G.W.T., J.M.L., R.B.C., and B.M.L. analyzed data; and R.R.-E., R.B.C., and B.M.L. wrote the paper.

The authors declare no conflict of interest.

‡To whom correspondence may be addressed. E-mail: croteau@wsu.edu or lange-m@wsu.edu.

This article contains supporting information online at www.pnas.org/cgi/content/full/0712314105/DC1.

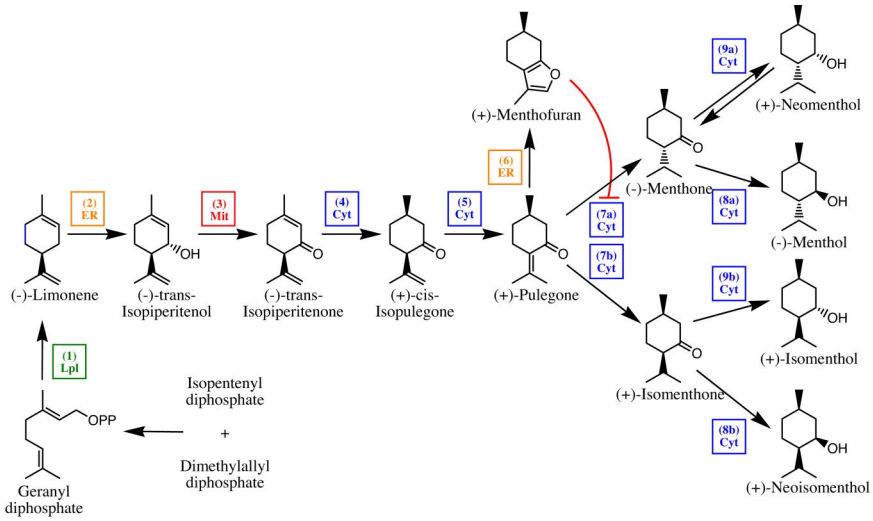

Fig. 1. Outline of *p*-menthane monoterpene metabolism in peppermint glandular trichomes. The following enzymes are involved in this pathway: indicated by ''(1),'' (−)-limonene synthase; indicated by ''(2),'' (−)-limonene 3-hydroxylase; indicated by ''(3),'' (−)-*trans*-isopiperitenol dehydrogenase; indicated by ''(4),'' (−)-*trans*-isopiperitenone reductase; indicated by ''(5),'' (+)-*cis*-isopulegone isomerase; indicated by ''(6),'' (+)-menthofuran synthase; indicated by ''(7a),'' (+)-pulegone reductase [(−)-menthone-forming activity]; indicated by ''(7b),'' (+)-pulegone reductase [(+)-isomenthone-forming activity]; indicated by ''(8a),'' (−)-menthone: (−)-menthol reductase [(−)-menthol-forming activity]; indicated by ''(8b),'' (−)-menthone: (−)-menthol reductase [(+)-neoisomenthol-forming activity]; indicated by ''(9a),'' (−)-menthone: (+)-neomenthol reductase [(+)-neomenthol-forming activity]; indicated by ''(9b),'' (−)-menthone: (+)-neomenthol reductase [(+)-isomenthol-forming activity]. The subcellular compartmentation of *p*-menthane metabolic enzymes is color-coded: Cyt (blue), cytosol; ER (orange), endoplasmic reticulum; Lpl (green), leucoplasts; Mit (red), mitochondria. The inhibition of PR by (+)-menthofuran, as demonstrated in the present manuscript, is indicated by a red arc with an orthogonal red line.

presence of (+)-menthofuran, thus resulting in a decreased PR activity and increased (+)-pulegone amounts (28). Because of these regulatory complexities and the occurrence of branch-points, the fine-tuning of monoterpene biosynthesis cannot be understood intuitively. Here, we report on the development of a kinetic mathematical model, based on the available experimental data, that accurately describes the behavior of the peppermint monoterpene biosynthetic pathway under various experimental conditions. Model predictions were used to generate nontrivial, testable hypotheses regarding poorly understood regulatory mechanisms, and modeling-guided follow-up experiments were used to demonstrate an as yet unidentified role for (+)-menthofuran as a competitive inhibitor of PR. These results indicate that gene expression and posttranslational modulation of enzyme activity both are important factors in regulating peppermint monoterpene biosynthesis.

Results and Discussion

Development of a Mathematical Model Simulating Monoterpene Biosynthesis in Peppermint Oil-Gland Secretory Cells. The filling of peppermint glandular trichomes with monoterpenoid essential oil is a complex process. A mathematical model simulating this process needs to account for various levels of regulation. Several estimates were made to allow linking microscopic variables (e.g., monoterpene composition in individual glandular trichomes) with macroscopic measurements (e.g., leaf monoterpene composition). The number of glandular trichomes per leaf depends on environmental and developmental parameters. Under greenhouse conditions, the number of biosynthetically active glandular trichomes increases from ≈2,500 (at day 5 after leaf initiation) to ≈13,000 (at day 18 after initiation) (ref. 29 and R.R.-E., G.W.T., and B.M.L., unpublished data), whereas under reduced light intensity (300 μmol m^{-2} s^{-1}), the maximum number of glandular trichomes is ≈7,500 (30) [details in supporting information (SI) *Appendix*]. The volume of the cluster of eight secretory cells of each individual glandular trichome, which does not depend on environmental conditions, can be determined based on microscopic size measurements (average diameter of the secretory cell disk is 60 μm, height is 16 μm). We approximated the shape of the secretory cell cluster as a frustum of a cone, the volume of which can be calculated as $\frac{1}{3}\,\pi\,h\,(R^2 + R\,r + r^2)$, thus resulting in a calculated average secretory cell disk volume of 2.35×10^{-5} μl at maturity. Morphometric measurements taken by using microscopic images at different developmental stages were combined with stereological approaches (31) to calculate the volume densities of subcellular compartments in peppermint oil-gland secretory cells, thus allowing us to estimate concentrations of enzymes based on prior knowledge regarding their organellar distribution (details in *SI Appendix*). We used two independent methods to calculate the amounts of monoterpenes produced per individual glandular trichome. First, monoterpene amounts obtained from gas chromatography–flame ionization detection (GC-FID) analyses of steam-distilled leaves were divided by the number of oil-bearing glandular trichomes. Second, the volume of the essential oil-filled subcuticular cavity of mature glandular trichomes was calculated based on the approximation of its shape as a hemisphere ($\frac{2}{3}\,\pi\,r^3$) with a diameter of 65 μm (determined with morphometric measurements taken by using microscopic images). The volume (7.53×10^{-5} μl) was then multiplied by the known essential oil density (0.9 mg/μl) to obtain the monoterpene amount per gland. An average monoterpene molecular weight of 150 g/mol was assumed for converting these values into molar amounts per gland (for details, see *SI Appendix*). Both approaches yielded very similar results with monoterpene amounts between 470 and 570 pmol per gland at maturity, indicating that the essential oil in peppermint glandular trichomes consists almost exclusively of monoterpenes.

Kinetic constants for monoterpene biosynthetic enzymes were obtained from the literature (11, 15, 17–19, 32). Michaelis–Menten rate equations were used to describe the kinetic behavior of individual biosynthetic enzymes. These expressions were used in a set of ordinary differential equations to account for the time dependence of the metabolite concentration (details in

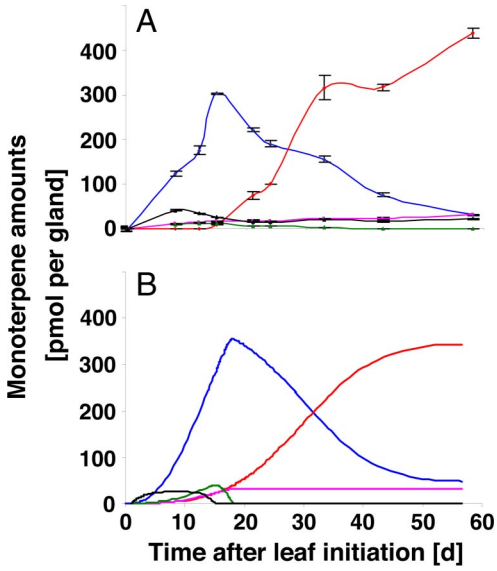

Fig. 2. Experimentally determined monoterpene profiles of peppermint plants grown under greenhouse conditions (*A*) and computer simulation based on a kinetic mathematical model of mint monoterpene biosynthesis (*B*). The following colors are used for indicating monoterpene profiles: black, (−)-limonene; pink, (+)-pulegone; green, (+)-menthofuran; blue, (−)-menthone; red, (−)-menthol.

SI Appendix). In addition, we accounted for changes in enzyme concentration during the course of leaf development by approximating the shape of previously reported enzyme activity patterns (22) with Gaussian functions (details in *SI Appendix*). We did not account for diurnal changes in enzyme activities and the effects of day/night temperature changes on enzyme kinetics; thus, the kinetic and enzyme activity values in our model represent "daily averages." A dynamic simulation of monoterpene profiles was performed by simultaneously solving the system of modified ordinary differential equations (expressing both enzyme properties and expression patterns) by using the ode15s function of the MATLAB software package. Because enzyme concentrations and the variables used for the Gaussian function representing developmental enzyme activity patterns could only be estimated, iterative optimizations of the initial model parameters were performed by using the experimentally measured monoterpene profiles as constraints, until the best fit of modeling results and experimental data were achieved. Our modeling simulated an early accumulation of high levels of (−)-menthone (maximum at 15 days), which is converted to (−)-menthol during the essential oil maturation phase (15–55 days), a transient low-level accumulation of (−)-limonene and (+)-pulegone, and a sigmoidal time course of (+)-menthofuran accumulation (low levels). These simulations were in excellent agreement with monoterpene profiles obtained with greenhouse-grown plants (Fig. 2). The fact that monoterpene profiles under regular growth conditions could be simulated successfully by considering only the kinetic properties and developmental expression patterns of biosynthetic enzymes confirmed previous conclusions that monoterpene biosynthesis is determined by the rate of biosynthesis (21), most likely regulated at the level of gene expression (22).

Mathematical Modeling Suggests that Posttranslational Regulation Determines Monoterpene Profiles Under Environmental Stress Conditions. Peppermint oil of the highest commercial quality can only be produced with plants grown in certain geographical regions with hot days and cool nights. It has also been known for many years that essential oil yield and composition vary widely among growing regions and are affected by numerous environmental and agronomic factors (reviewed in ref. 33). To evaluate the suitability of mathematical modeling for understanding environmental effects on essential oil biosynthesis, we subjected peppermint plants to a series of environmental stresses, measured monoterpene profiles, and tested several hypotheses regarding biochemical and regulatory mechanisms underlying the accumulation of undesirable essential oil components, in particular (+)-pulegone and (+)-menthofuran, based on the degree of convergence between these experimental data and computational simulations. Under all environmental conditions tested (reduction of water/fertilizer to 50%, lowering of light intensity, or increase of night temperatures), a reduction of total oil yield was measured, which correlated with smaller leaves and a lower number of glandular trichomes per leaf (R.R.-E., G.W.T., and B.M.L., unpublished results). In certain experiments (low light and high night temperatures), we also detected an accumulation of (+)-pulegone and (+)-menthofuran (data not shown), the simulation of which required testing various hypotheses computationally. Here, we are going to use the low-light experiment as an example to illustrate the process of computational hypothesis testing.

Control plants were grown in a greenhouse with additional lighting from sodium-vapor lights (850 μmol m^{-2} s^{-1} of photosynthetically active radiation), a 16-h photoperiod and a temperature cycle of 27°C/21°C (day/night), whereas the experimental treatment involved plants kept in a growth chamber at reduced light intensity (300 μmol m^{-2} s^{-1} of photosynthetically active radiation) but under otherwise identical conditions as controls. Total essential oil yield was ≈50% lower in plants grown under low light conditions (480–630 μg per leaf at maturity) compared with controls (1,160–1,270 μg per leaf at maturity) (Fig. 3*A*). Cultivation under low-light conditions led to a transient increase of (+)-pulegone, with a maximum of 70 pmol per glandular trichome at 18 days and a hyperbolic accumulation of (+)-menthofuran of ≈60 pmol per glandular trichome. Mahmoud and Croteau have reported that (+)-pulegone and (+)-menthofuran increased and decreased, respectively, in concert under stress conditions (27, 28). Stem-feeding experiments with (+)-menthofuran led to a dose-dependent decrease in the expression of the gene encoding PR, the enzyme responsible for the conversion of (+)-pulegone into (−)-menthone, by an as yet unidentified mechanism (28). Furthermore, in transgenic lines with increased expression levels of the gene encoding MFS and higher (+)-menthofuran amounts in the essential oil, (+)-pulegone amounts were higher than in controls, which led to the hypothesis that the metabolic fate of (+)-pulegone is controlled by a (+)-menthofuran-mediated transcriptional down-regulation of PR levels (28). To test whether these assumptions could guide simulations of the monoterpene profiles observed in the present experiments with low-light-grown plants, we initially increased the levels of MFS and decreased PR levels (2-fold up and 2-fold down, respectively) in our mathematical model (*SI Appendix*). Simulations using these model adjustments indicated that, compared with controls, the peak levels of (+)-pulegone and (+)-menthofuran should be dramatically increased (160 and 150 pmol per gland, respectively), whereas (−)-menthone and (−)-menthol levels would be drastically reduced (190 and 220 pmol per gland, respectively) (Fig. 3*B*). We then simulated numerous other reasonable combinations with increased MFS and decreased PR levels (1.5- to 2.5-fold up and down, respectively), but a satisfactory simulation of the measured monoterpene profiles could not be obtained. Because these simulations were only in partial agreement with experimentally determined values, alternative hypotheses regarding the biochemical mechanisms of environmental variation in peppermint essential oil composition had to be considered.

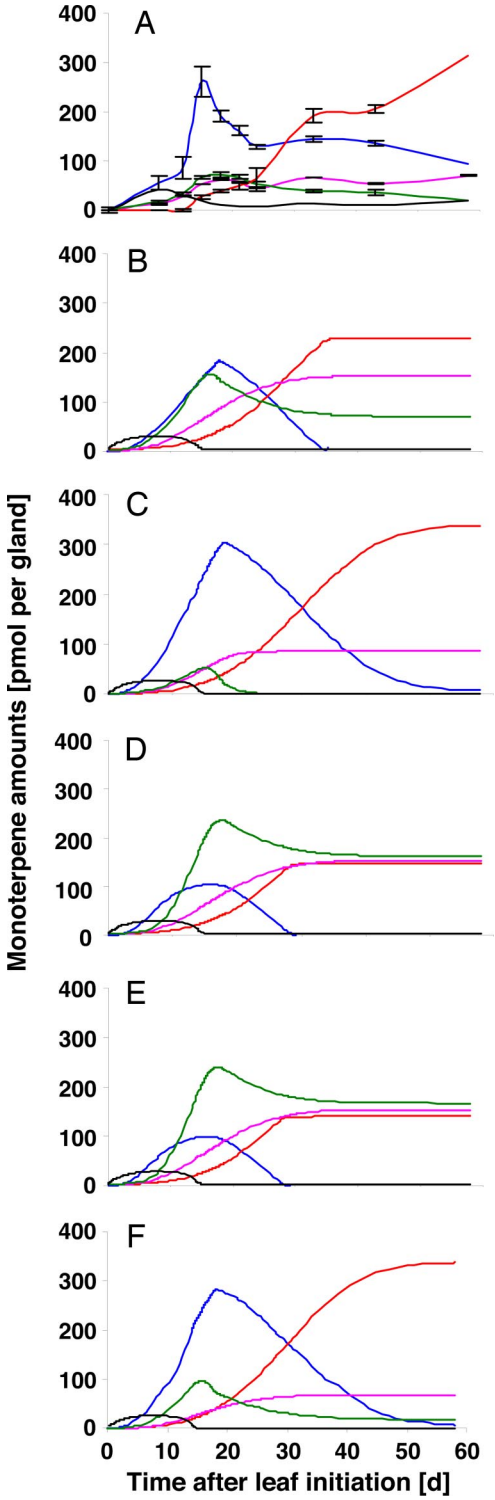

Fig. 3. Effect of stress on monoterpene metabolism. Monoterpene profiles of peppermint plants maintained in growth chambers under low-light conditions (*A*) and computer simulation considering a reduction of PR and increase in MFS transcript levels (as suggested in ref. 28) (*B*). Simulations assuming an inhibition of PR by (+)-menthofuran by a competitive (*C*), uncompetitive (*D*) or noncompetitive (*E*) mechanism. Simulation of monoterpene profiles under low-light conditions after model optimization (*F*). Color-coding of monoterpene profiles is as in Fig. 2.

As a plausible and as yet unexplored possibility for peppermint monoterpene pathway regulation, we simulated the essential oil composition if inhibitory effects of (+)-menthofuran on PR were assumed. Using our model, we tested for competitive, uncompetitive, and noncompetitive inhibition by using assumed K_i values of 10 μM (Matlab code in *SI Appendix*). Simulations assuming a competitive inhibition mechanism were in excellent agreement with monoterpene values measured experimentally (Fig. 3*C*), whereas simulations for uncompetitive or noncompetitive inhibition of PR by (+)-menthofuran predicted very high accumulation levels for (+)-pulegone and (+)-menthofuran (Fig. 3 *D* and *E*). Based on these computational predictions, we then tested experimentally whether (+)-menthofuran exerted inhibitory effects on PR activity.

(+)-Menthofuran Is a Competitive Inhibitor of PR. Recombinant PR was expressed in *Escherichia coli*, partially purified, and assayed as described previously (17). The kinetic constants we determined for (+)-pulegone as a substrate [K_m = 40 μM, V_{max} = 185 pmol/s, and IC_{50} (substrate inhibition) = 150 μM] were very similar to those reported previously, although our K_m value was a bit higher (17). After completing these preliminary studies to establish the appropriate assay conditions, PR enzyme activity was measured with (+)-pulegone as a substrate (0–100 μM), NADPH as a cofactor (500 μM), and varying concentrations of the putative inhibitor (+)-menthofuran (0–400 μM). We observed a dose-dependent decrease in PR activity in the presence of (+)-menthofuran (Fig. 4*A*). To evaluate the mechanism of inhibition, we used the Lineweaver–Burk method (34), in which $1/V$ (V = velocity) is plotted against 1/[S] ([S] = substrate concentration) (Fig. 4*B*). The lines obtained for different inhibitor concentrations had a common intercept with the $1/V$ axis, but the slopes of the lines increased with rising inhibitor concentrations. The V_{max} value (determined based on intercept with the $1/V$ axis) remained the same in the presence of different inhibitor amounts, whereas the K_m value (determined based on the intercept with the 1/[S] axis) increased with rising inhibitor concentrations, thus indicating a competitive inhibition mechanism. The inhibition constant (K_i), which defines the competition of substrate and inhibitor for the same active site of PR, was determined by using two independent approaches: (*i*) with the Dixon method (plotting $1/V$ against [I] ([I] = inhibitor concentration), K_i was determined by linear regression analysis (35); and (*ii*) with the $K_{m(app)}$ method (plotting $K_{m(app)}/V_{max}$ against [I]), K_i was obtained by a nonlinear regression analysis (36). In both cases, a K_i for (+)-menthofuran as a competitive inhibitor of ≈300 μM was calculated. Using the same methods, we estimated a K_i of 112 μM for substrate inhibition by (+)-pulegone. Because (+)-menthofuran appeared to be a relatively weak competitive inhibitor [K_i value for (+)-menthofuran ≈7.5-fold higher than the K_m value for (+)-pulegone as substrate], we tested whether (+)-menthofuran concentrations in peppermint secretory cells were sufficiently high to give rise to relevant inhibitory effects.

(+)-Menthofuran Is Preferentially Retained in Peppermint Oil-Gland Secretory Cells. Leaves from greenhouse-grown peppermint plants were harvested at 20 and 50 days, secretory cells were isolated and steam distilled, and monoterpene profiles were analyzed by GC-FID (modified from ref. 17). Secretory cells from plants grown in the greenhouse contained primarily (−)-menthone at 20 days and substantial amounts of (−)-menthol at 50 days, whereas only small amounts of (+)-menthofuran and negligible amounts of (+)-pulegone were detected (details in *SI Appendix*). In contrast, secretory cells obtained from plants grown under stress conditions (low light intensity) accumulated (+)-menthofuran as the principal metabolite (up to 20 mM, accounting to ≈90% of total monoterpenes). High amounts of (+)-menthofuran had been detected in secretory cells previously when grown under comparable growth conditions (3), but it had not been recognized that this was due to stress conditions (low

BIOCHEMISTRY

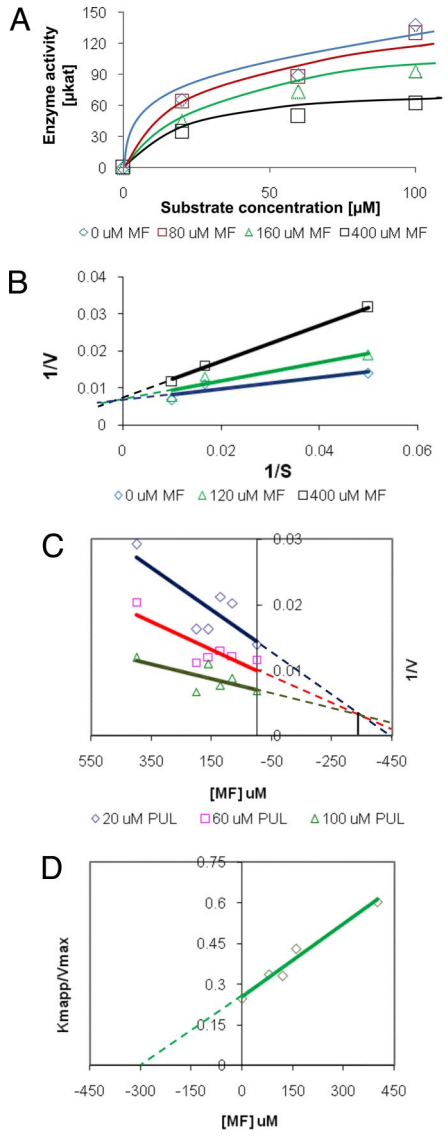

Fig. 4. Characterization of (+)-menthofuran as a competitive inhibitor of peppermint PR. (*A*) Effect of various (+)-menthofuran concentrations on PR activity. (*B*) Lineweaver–Burk plot for determining the type of inhibition exerted. Determination of the inhibition constant for (+)-menthofuran by using a Dixon plot (*C*) and a nonlinear regression analysis (*D*). The graphs are based on triplicate assays and three independent experiments.

light intensity). When we obtained essential oil directly from the subcuticular storage cavity of intact glandular trichomes by using microcapillaries and analyzed it by GC-FID, the monoterpene profile was similar to that of steam-distilled whole leaves (low amounts of (+)-menthofuran in greenhouse-grown plants and moderate amounts in stressed plants) (data not shown). These results indicated that (+)-menthofuran was preferentially retained in secretory cells under stress conditions. Based on these findings, our mathematical model was updated to reflect the experimentally determined kinetic properties of PR [$K_{m(+)\text{-pulegone}} = 40\ \mu M$; $K_{i(+)\text{-pulegone}} = 112\ \mu M$ (by introducing a factor q the percentage of the the total PR activity affected by substrate inhibition can be adjusted); $K_{i(+)\text{-menthofuran}} = 300\ \mu M$ (by introducing a factor p the percentage of the total PR activity affected by (+)-menthofuran inhibition can be adjusted)] and the high intracellular concentration of (+)-menthofuran [by introducing a factor z the local concentration of (+)-menthofuran can be adjusted]. Simulations of low-light conditions (Fig. 3*E*) were in excellent agreement with experimentally determined monoterpene profiles. By using this second-generation model, different environmental conditions can now be simulated by simply modifying a set of variable factors. Our simulations also have the potential of enabling knowledge-based metabolic engineering approaches aimed at modulating monoterpene yield and composition. An improved understanding of the transport processes involved in monoterpenoid essential oil biosynthesis and secretion will be a key future challenge for advancing our simulation efforts.

Materials and Methods

Plant Material. Peppermint (*Mentha* × *piperita* cv. Black Mitcham) plants were grown on soil (Sunshine Mix LC1; SunGro Horticulture) in a greenhouse with supplemental lighting from sodium-vapor lights (850 μmol m^{-2} s^{-1} of photosynthetically active radiation at plant canopy level) with a 16-h photoperiod and a temperature cycle of 27°C/21°C (day/night). Plants were watered daily with a fertilizer mix (N:P:K 20:20:20, wt/wt/wt; plus iron chelate and micronutrients). Monoterpene analyses were performed with leaves that were initiated on 3-week-old stems and were harvested at ages ranging from 5 to 55 days after bud formation. Stress experiments were performed by moving plants to a growth chamber with a 16-h photoperiod at reduced light levels (300 μmol m^{-2} s^{-1} of photosynthetically active radiation at plant-canopy level).

Monoterpene Analysis. Leaves and isolated secretory cells (37) were directly (without prior freezing) steam-distilled and solvent-extracted by using 10 ml of pentane in a condenser-cooled Likens–Nickerson apparatus (17). Monoterpenes were identified by comparison of retention times and mass spectra to those of authentic standards in gas chromatography with mass spectrometry detection. Quantification was achieved by gas chromatography with flame ionization detection (17) based on calibration curves with known amounts of authentic standards and normalization to the peak area of camphor as internal standard.

Morphometric Measurements. The volume of the secretory cells and subcuticular cavity of peppermint secretory cells, as well as the volume densities of subcellular compartments within secretory cells, were estimated based on the morphometric and stereological approaches outlined in refs. 30 and 31. A detailed description of measurements, assumptions, and calculations are provided in *SI Appendix*.

Kinetic Modeling and Simulation. A kinetic mathematical model was developed to simulate monoterpene profiles based on prior knowledge of enzyme expression patterns and kinetic properties. Detailed descriptions of our modeling approaches and the MATLAB source code, in compliance with the Minimal Information Requested in the Annotation of Biochemical Models (MIRIAM) guidelines for annotating biochemical models (38), are provided in *SI Appendix*.

Cell-Free Assaying of Recombinant PR Activity and Inhibition Experiments. *E. coli* BL21(DE3) cells (Invitrogen) were individually transformed with the pSBET plasmids containing peppermint PR cDNA clone ml579 (AY300163). Transformed *E. coli* cells were grown, recombinant protein production induced, cells harvested, and recombinant protein extracted and partially purified according to ref. 15. Routine enzyme assays contained 100 μM (+)-pulegone, 500 μM NADPH, and 9.2 μg of total protein in 100 μl of 50 mM MOPSO (pH 6.6). Reaction times were adjusted to ensure that no more than 20% of the available substrate was consumed. Enzymatic reactions were terminated by vortexing with 0.5 ml of pentane and an aliquot of the organic extract was analyzed by GC-FID as above. Kinetic parameters were determined by varying substrate concentration while maintaining other reactants at saturation. Kinetic constants (K_m and V_{max}) were calculated by nonlinear regression analysis (Origin 6.0; OriginLab). Substrate inhibition was evaluated in triplicate assays using 15 different (+)-pulegone concentrations between 10 and 800 μM. Preliminary assays to test inhibitory effects on PR activity were performed by using varying amounts of (+)-pulegone and (+)-menthofuran (15 different concentrations between 0 and 800 μM). Triplicate assays were then performed with 0, 20, 60, and 100 μM (+)-pulegone and 0, 80, 160, and 400 μM (+)-menthofuran. Based on these data, the mechanism of inhibition was assessed graphically by using a Lineweaver–Burk plot (34). The inhibition

constant (*Ki*) for (+)-menthofuran was determined by using the Dixon method (35) and nonlinear regression analysis (36).

ACKNOWLEDGMENTS. We thank Julia Gothard-Szamosfalvi and Greg Whitney for growing plants, Dr. Ed Davis for valuable discussions and experimental advice, and Iris Lange for technical assistance. R.R.-E. thanks the Fulbright Program and the University of Antioquia (Medellin, Colombia) for scholarships. This work was supported in part by Agricultural Research Center Grants (to B.M.L. and R.B.C.) and the Mint Industry Research Council Grant (to R.B.C.).

1. Lawrence BM (1981) in *Essential Oils* (Allured, Wheatin, IL), pp 1–81.
2. Gershenzon J, Maffei M, Croteau R (1989) Biochemical and histochemical localization of monoterpene biosynthesis in the glandular trichomes of spearmint (*Mentha spicata*). *Plant Physiol* 89:1351–1357.
3. McCaskill D, Gershenzon J, Croteau R (1992) Morphology and monoterpene biosynthetic capabilities of secretory cell clusters isolated from glandular trichomes of peppermint (*Mentha* × *piperita* L.). *Planta* 187:445–454.
4. Amelunxen F, Wahlig T, Arbeiter H (1969) Detection of essential oil in isolated glandular trichomes of *Mentha piperita* L (Translated from German). *Pflanzenphysiol* 61:68–72.
5. Amelunxen F (1965) Electron microscopy analysis of glandular trichomes of *Mentha piperita* L (Translated from German). *Planta Med* 13:457–473.
6. Gershenzon J, *et al.* (1992) Isolation of secretory cells from plant glandular trichomes and their use in biosynthetic studies of monoterpenes and other gland products. *Anal Biochem* 200:130–138.
7. Lange BM, *et al.* (2000) Probing essential oil biosynthesis and secretion by functional evaluation of expressed sequence tags from mint glandular trichomes. *Proc Natl Acad Sci USA* 97:2934–2939.
8. Croteau R, Davis EM, Ringer KL, Wildung MR (2005) (−)-Menthol biosynthesis and molecular genetics. *Naturwiss* 92:562–577.
9. McCaskill D, Croteau R (1995) Monoterpene and sesquiterpene biosynthesis in glandular trichomes of peppermint (*Mentha* × *piperita*) rely exclusively on plastid-derived isopentenyl diphosphate. *Planta* 197:49–56.
10. Eisenreich W, Sagner S, Zenk MH, Bacher A (1997) Monoterpenoid essential oils are not of mevalonoid origin. *Tetrahedron Lett* 38:3889–3892.
11. Alonso WR, Rajaonarivony JIM, Gershenzon J, Croteau R (1992) Purification of 4*S*-limonene synthase, a monoterpene cyclase from the glandular trichomes of peppermint (*Mentha* × *piperita*) and spearmint (*M. spicata*). *J Biol Chem* 267:7582–7587.
12. Colby SM, Alonso WR, Katahira E, McGarvey DJ, Croteau R (1993) 4*S*-Limonene synthase from the oil glands of spearmint (*Mentha spicata*): cDNA isolation, characterization and bacterial expression of the catalytically active monoterpene cyclase. *J Biol Chem* 268:23016–23024.
13. Turner G, Gershenzon J, Nielson EE, Froehlich JE, Croteau (1999) Limonene synthase, the enzyme responsible for monoterpene biosynthesis in peppermint, is localized to leucoplasts of oil-gland secretory cells. *Plant Physiol* 120:879–886.
14. Lupien S, Karp F, Wildung MR, Croteau R (1999) Regiospecific cytochrome P450 limonene hydroxylases from mint (*Mentha*) species: cDNA isolation, characterization, and functional expression of (−)-4*S*-limonene-3-hydroxylase and (−)-4*S*-limonene-6-hydroxylase. *Arch Biochem Biophys* 368:181–192.
15. Ringer KL, Davis EM, Croteau R (2005) Monoterpene metabolism: cloning, expression and characterization of (−)-isopiperitenol/(−)-carveol dehydrogenase from peppermint and spearmint. *Plant Physiol* 137:863–872.
16. Turner GW, Croteau R (2004) Organization of monoterpene biosynthesis in *Mentha*: Immunocytochemical localization of geranyl diphosphate synthase, limonene-6-hydroxylase, isopiperitenol dehydrogenase, and pulegone reductase. *Plant Physiol* 136:4215–4227.
17. Ringer KL, McConkey ME, Davis EM, Rushing GW, Croteau R (2003) Monoterpene double-bond reductases of the (−)-menthol biosynthetic pathway: Isolation and characterization of cDNAs encoding (−)-isopiperitenone reductase and PR of peppermint. *Arch Biochem Biophys* 418:80–92.
18. Kjonaas RB, Venkatachalam KV, Croteau R (1985) Metabolism of monoterpenes: Oxidation of isopiperitenol to isopiperitenone, and subsequent isomerization to piperitenone, by soluble enzyme preparations from peppermint (*Mentha piperita*) leaves. *Arch Biochem Biophys* 238:49–60.
19. Davis EM, Ringer KL, McConkey ME, Croteau R (2005) Monoterpene metabolism: Cloning, expression and characterization of menthone reductases from peppermint. *Plant Physiol* 137:873–881.
20. Bertea CM, Schalk M, Karp F, Maffei M, Croteau R (2001) Demonstration that menthofuran synthase of mint (*Mentha*) is a cytochrome P450 monooxygenase: Cloning, functional expression and characterization of the responsible gene. *Arch Biochem Biophys* 390:279–286.
21. Gershenzon J, McConkey ME, Croteau R (2000) Regulation of monoterpene accumulation in leaves of peppermint (*Mentha* × *piperita* L.). *Plant Physiol* 122:205–214.
22. McConkey ME, Gershenzon J, Croteau R (2000) Developmental regulation of monoterpene biosynthesis in the glandular trichomes of peppermint (*Mentha* × *piperita* L.). *Plant Physiol* 122:215–233.
23. Guenther E (1972) *The Essential Oils, Vol I–VI* (Krieger, Huntington, NY).
24. Court WA, Roy RC, Pocs R (1993) Effect of harvest date on the yield and quality of the essential oil of peppermint. *Can J Plant Sci* 73:815–824.
25. Burbott AJ, Loomis WD (1967) Effects of light and temperature on the monoterpenes of peppermint. *Plant Physiol* 42:20–28.
26. Clark RJ, Menary RC (1980) Environmental effects on peppermint, I. Effect of day length, photon flux density, night temperature and day temperature on the yield and composition of peppermint oil. *Aust J Plant Physiol* 7:685–692.
27. Mahmoud SS, Croteau RB (2001) Metabolic engineering of essential oil yield and composition in mint by altering expression of deoxyxylulose phosphate reductoisomerase and menthofuran synthase. *Proc Natl Acad Sci USA* 98:8915–8920.
28. Mahmoud SS, Croteau RB (2003) Menthofuran regulates essential oil biosynthesis in peppermint by controlling a downstream monoterpene reductase. *Proc Natl Acad Sci USA* 100:14481–14486.
29. Colson M, Pupier R, Perrin A (1993) Biomathematical analysis of the number of glandular trichomes on leaves of *Mentha* × *piperita* (Translated from French). *Can J Bot* 71:1202–1211.
30. Turner GW, Gershenzon J, Croteau R (2000) Distribution of peltate glandular trichomes on developing leaves of peppermint (*Mentha* × *piperita* L.). *Plant Physiol* 124:655–664.
31. Weibel ER (1979) in *Stereological Methods, Vol 1, Practical Methods for Biological Morphometry*, ed Weibel ER (Academic, London), pp 63–100.
32. Karp F, Mihaliak CA, Harris JL, Croteau R (1990) Monoterpene biosynthesis: Specificity of the hydroxylations of (−)-limonene by enzyme preparations from peppermint (*Mentha piperita*), spearmint (*Mentha spicata*), and perilla (*Perilla frutescens*) leaves. *Arch Biochem Biophys* 276:219–226.
33. Lawrence BM (2006) *Mint: The Genus Mentha*. (CRC, Boca Raton, FL).
34. Lineweaver H, Burk D (1934) The determination of enzyme dissociation constants. *J Am Chem Soc* 56:658–666.
35. Dixon M (1952) The determination of enzyme inhibitor constants. *Biochem J* 55:170–171.
36. Kakkar T, Boxenbaum H, Mayersohn M (1999) Estimation of K_i in a competitive enzyme-inhibition model: Comparisons among three methods of data analysis. *Drug Metab Dispos* 27:756–762.
37. Gershenzon J, *et al.* (1992) Isolation of secretory cells from plant glandular trichomes and their use in biosynthetic studies of monoterpenes and other gland products. *Anal Biochem* 200:130–138.
38. Le Novère N, *et al.* (2005) Minimum information requested in the annotation of biochemical models (MIRIAM). *Nat Biotechnol* 23:1509–1515.